

Droplet condensation in turbulent flows

A. CELANI¹, G. FALKOVICH², A. MAZZINO³ and A. SEMINARA^{1,3}

¹ *CNRS, INLN - 1361 Route des Lucioles, 06560 Valbonne, France*

² *Physics of Complex Systems, Weizmann Institute of Science - Rehovot 76100, Israel*

³ *INFM, Dipartimento di Fisica, Università degli Studi di Genova and INFN, Sezione di Genova - Via Dodecaneso 33, 16146 Genova, Italy*

received 28 January 2005; accepted in final form 19 April 2005

published online 25 May 2005

PACS. 47.27.Eq – Turbulence simulation and modeling.

PACS. 47.27.Gs – Isotropic turbulence; homogeneous turbulence.

Abstract. – The problem of droplet growth by condensation in a turbulent flow of nearly saturated vapour is addressed theoretically and numerically. We show how the presence of an underlying turbulent velocity field induces a correlation between droplet trajectories and supersaturation. This leads both to the enhancement of the droplet growth rate and to a fast spreading of the droplet size distribution.

Introduction. – The evolution of microdroplets in a turbulent environment is an issue of great interest for a variety of applications ranging from health care [1], to engineering, to atmospheric sciences [2–4]. In the latter context, microdroplet growth by condensation/evaporation is a phenomenon of paramount importance for the early stages of cloud evolution. Warm clouds are essentially a polydisperse aerosol of water droplets suspended in a moist air. The smallest droplets are created by condensation onto sub-micron solid particles (cloud condensation nuclei), whereas raindrops typically exceed 1 mm in radius. This observation naturally motivates one to investigate droplet growth, which eventually leads droplets to fall under gravitational force. Different stages follow droplets formation. First, they grow by condensation of vapour molecules on their surface. Second, upon having reached a radius of the order of 20 μm , they begin to coalesce to form bigger drops. Here we focus on the first stage of the growth by condensation. Experimental measurements of droplet radii (see, *e.g.*, [5, 6]) in fair weather clouds show a broad distribution in the range 1–20 μm . The presence of droplets with very different sizes can significantly enhance the efficiency of successive collisions and thus contribute to a fast initiation of the precipitation process. However, up to now this effect has not been reproduced by classical models of the condensation stage [7]. Their basic ingredient is the assumption that droplets are essentially confined to a small portion of the cloud, dubbed “fluid parcel”, where they experience the same value of humidity. Many efforts have been made to evaluate the influence of fine scale turbulence on the macroscopic properties of clouds (see [8] for a review). Recent numerical simulations of a turbulent ascending moist air parcel show that resolving the fluctuations below the scale of the parcel itself does not result in a significant spectral broadening [9–11]. The theory assuming Brownian random walk of an air

parcel in a vertical gradient of humidity does not give much broadening too [12]. Here we use a straightforward approach considering air velocity and vapour concentration as fields in space and evaluate droplet distribution in such a strongly fluctuating system. We thus consider the fundamental problem of a turbulent flow \mathbf{v} which advects a vapour field and a number of droplets. Cloud physics is discussed as one of the possible applications of this analysis.

The idea is that the simultaneous transport of droplets and vapour by the same velocity field induces correlations between droplet trajectories and supersaturation values. Such correlation allows droplets to experience the same supersaturation value for a very long time. Let us stress that we do not consider edge effects like entrainment of dry air; the fluctuations of supersaturation are produced inside the cloud by the turbulent velocity field acting on the vertical gradient of humidity sustained by temperature. Strong fluctuations of humidity and the correlation between droplet trajectories and supersaturation lead to a significant spreading of the distribution of droplets radii.

In this letter we perform direct numerical simulations of the evolution of droplet trajectories and radii and of the velocity and supersaturation fields. We show a relevant effect of correlation induced by turbulent transport which reproduces a remarkable spreading of the size distribution. Droplets and water vapour molecules are the protagonists of this peculiar process. We discuss the possible impact of these ideas for condensation in clouds.

Model and DNS. – We consider the simplest generalization of the one-dimensional Twomey's model [13]. Twomey considered every droplet to grow in the same humidity conditions, while we consider the presence of vapour to vary in space and time. For this reason we introduce the supersaturation field $s(\mathbf{x}, t) := \frac{e}{e_s}(\mathbf{x}, t) - 1$, where e and e_s are the vapour pressure and the saturation vapour pressure, respectively. $s(\mathbf{x}, t)$ quantifies the amount of vapour which is present in point \mathbf{x} at time t : droplets are able to grow only where s is positive, that is in moist air (see eq. (3)). On the contrary, droplets tend to evaporate where s is negative (dry regions). The field s is taken as a passive scalar transported by a homogeneous turbulent flow $\mathbf{v}(\mathbf{x}, t)$ which is not affected by its presence. Here we assume that local fluctuations of e_s are small so that fluctuations in s can be considered as a sum of fluctuations in e and e_s . In addition, vapour diffusivity and thermodiffusivity are close which makes s approximately satisfying the advection-diffusion equation. These assumptions lead to the following dynamical equations:

$$\partial_t s + \mathbf{v} \cdot \nabla s = A_1 w - \frac{s}{\tau_s} + D \nabla^2 s, \quad (1)$$

$$\partial_t \mathbf{v} + \mathbf{v} \cdot \nabla \mathbf{v} = -\nabla p + \nu \nabla^2 \mathbf{v} + \mathbf{f}, \quad (2)$$

where w is the vertical component of the velocity field which obeys the Navier-Stokes equation (2). Let us remark that the passive scalar approximation for s can be applied in warm clouds, because here the parameters A_1 and τ_s depend very weakly on temperature⁽¹⁾. The effect of the vertical temperature gradient, which certainly affects the global circulation in a cloud, can be neglected upon focusing on a volume of some hundreds of meters (see [14]). As we will discuss later, we are interested in such volume (large but not the largest), where the homogeneous-isotropic turbulence scheme holds. In the advection-diffusion equation (1), A_1 is the steady vertical gradient of the supersaturation so that the term $A_1 w$ is a source of supersaturation due to adiabatic ascent and the term $-s/\tau_s$ is the loss of water vapour due to condensation on droplet surface [2]. The balance of the source and sink with mixing and

⁽¹⁾For warm-clouds temperatures, ranging from 273 to 300 K, we have A_1 ranging from $4.6E - 4 \text{ m}^{-1}$ to $5.7E - 4 \text{ m}^{-1}$, and (considering droplets of radius $10 \mu\text{m}$ and number density 100 cm^{-3}) τ_s ranging from 3.1 s to 3.2 s.

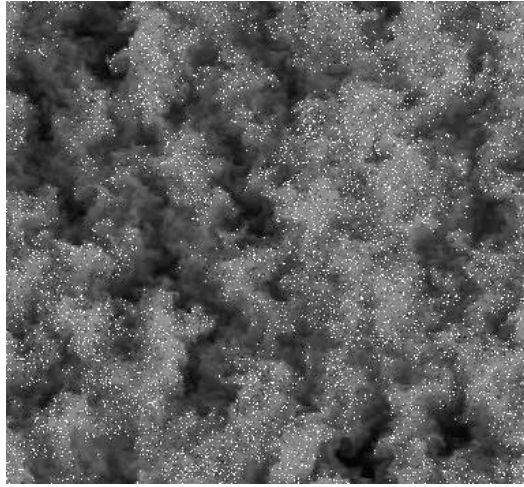


Fig. 1 – Spatial distribution of droplets (white points) and supersaturation field (light gray: supersaturated vapour $s > 0$, dark gray: subsaturated vapour $s < 0$). Droplets are preferentially concentrated in supersaturated portions of the cloud. This figure is obtained through a direct numerical simulation of a bi-dimensional domain $L \times L$. Evolution equations for velocity \mathbf{v} and supersaturation s are integrated by a pseudo-spectral code with second-order Runge-Kutta scheme for time marching and periodic boundary conditions, with initial conditions obtained by running a simulation for about 20 large-eddy turnover time, in order to obtain a steady state. The velocity field is in the inverse cascade regime and shows power spectra very close to Kolmogorov 1941 prediction. For the velocity field, the energy injected at an average rate ϵ by a small-scale random forcing is dissipated on large scales by a linear friction $-\alpha \mathbf{v}$. Also the scalar field is in a steady state of direct cascade forced by the velocity field component in the direction of gravity (see eq. (1)). The resolution is 1024^2 . Lagrangian equations (3), (4), (5) for $N = 20000$ droplet sizes and trajectories are integrated by an Euler method via bilinear interpolation of \mathbf{v} and s . For this value of N the term s/τ_s is negligible compared to other terms in eq. (1). We chose absorbing boundary conditions for R , *i.e.* a droplet whose size vanishes is abandoned, and no new particles are considered to enter the volume. Initially droplets are homogeneously distributed.

diffusion determines the equilibrium value of supersaturation fluctuations. The timescale τ_s (*absorption time*) parameterizes such absorption of supersaturation as discussed in [8]. Its value depends on the presence of droplets: $\tau_s^{-1} \propto n \int_0^\infty r P(r, t) dr$, where n is the numerical density of droplets, r is the value of droplet size and $P(r, t)$ is the size distribution. In the following analysis the sink term turns out to be negligible due to the smallness of n . This does not affect the qualitative behaviour of the supersaturation field. Equations (1), (2) are coupled with the Lagrangian evolution of droplet sizes R and trajectories \mathbf{X} :

$$\dot{R}(t) = A_3 s(\mathbf{X}(t), t) / R(t), \quad (3)$$

$$\dot{\mathbf{X}}(t) = \mathbf{U}(t) + \sqrt{2D} \boldsymbol{\eta}(t), \quad (4)$$

$$\dot{\mathbf{U}}(t) = -[\mathbf{v}(\mathbf{X}(t), t) - \mathbf{U}(t)] / \tau_d + g \hat{\mathbf{z}}, \quad (5)$$

where $\tau_d = r^2 / (3\nu\beta)$ is the Stokes timescale which characterizes every droplet⁽²⁾ ($\tau_d \approx 5 \cdot 10^{-4} - 8 \cdot 10^{-3}$ s for water droplets of radius $5-20 \mu\text{m}$ in air). Note that we consider isolated droplets because during the condensation stage interactions between droplets are negligible.

⁽²⁾ ν is the kinematic viscosity of air and $\beta = 3\rho_a / (2\rho_d + \rho_a)$.

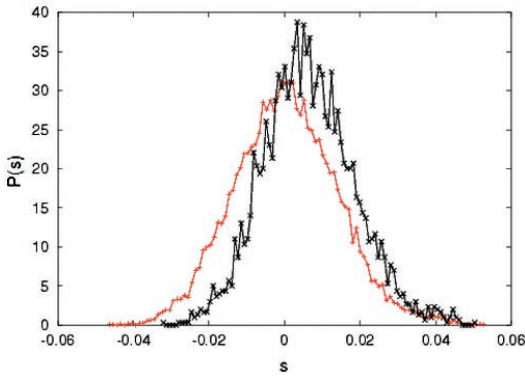


Fig. 2

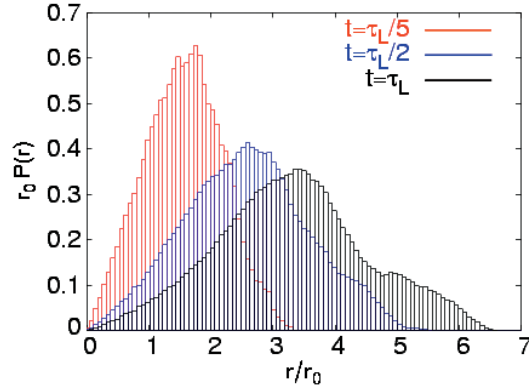


Fig. 3

Fig. 2 – Eulerian (gray, red on-line, curve) and Lagrangian (black curve) PDF of supersaturation at time $t = \tau_L$, where $\tau_L = \epsilon^{-1/3} L^{2/3}$ is the large-eddy turnover time.

Fig. 3 – Distribution $P(r)$ of droplet size r divided by the initial size r_0 , at times $\tau_L/5$, $\tau_L/2$ and τ_L . The droplet size spectrum evolution shows a relevant spreading, which, after one τ_L produces 40% of droplets with $r > 4r_0$.

Equation (3) with the expression for A_3 can be found in [2], it has been widely used in classical models for an air parcel rising adiabatically. However, in our model, the size growth rate varies from a droplet to another, because it corresponds to the supersaturation value calculated along the trajectory of the droplet. Due to turbulent dispersion initially close droplets will eventually experience disparate values of supersaturation. From fig. 1 we detect a segregation effect in the spatial distribution of droplets. This feature is due to the presence of turbulent correlations between droplets and water vapour which allow droplets to experience for a long time the same supersaturation fluctuation. Consequently, when they fall for a long time in a dry region (shown in blue on-line) they totally evaporate and disappear making dry regions void of particles. A quantitative evaluation of the presence of correlations can be done by comparing Lagrangian and Eulerian statistics of the supersaturation field. We verify that the supersaturation values experienced by cloud droplets are greater than expected on the basis of Eulerian statistics alone (see fig. 2).

In fig. 3 the evolution of size distribution in time is shown. As expected from the presence of the correlation shown in fig. 1, we observe a relevant spreading of the size distribution which qualitatively agrees with observations. At the end of the condensation stage we observe a population of droplets having very different sizes: large droplets spent a long time in the moist environment while droplets in dry air remained small (this is very important for cloud physics, as remarked at the very beginning).

The question which naturally arises now is whether large and small droplets coexist locally, in a small volume. This is a very important question for coalescence because collision and collection are enhanced by the presence of very different droplets only if they come close, otherwise they never meet. To address this issue we divide the computational domain in a grid of $M \times M$ non-overlapping boxes (for different values of M). Within every box we consider, at a fixed time, the size distribution of the local population and evaluate it as a function of the variable $R/\langle R \rangle_{box}$, where $\langle R \rangle_{box}$ is the local mean radius⁽³⁾. Then we average the M^2 local PDFs

⁽³⁾For $M = 1$ they reduce to the global spectrum (last curve in fig. 3) normalized to the global mean radius.

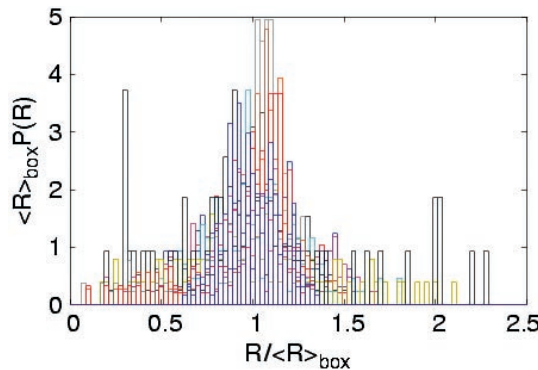


Fig. 4

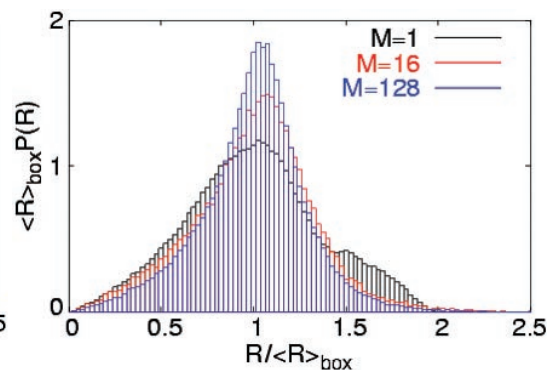


Fig. 5

Fig. 4 – Local distribution of droplet radii in 12 randomly picked boxes out of 4096 ($M = 64$) at time $t = \tau_L$.

Fig. 5 – PDF of droplet sizes averaged on M^2 boxes, for $M = 1, 16, 128$. We have excluded all boxes which contain only one particle. For the smallest boxes ($M = 128$) the number of almost void boxes, *i.e.* with one particle only, amounts to 3.6%. This value decreases upon increasing the total number of particles N . Here $N = 10^6$.

and compare the averages obtained for different M . In fig. 4 some of the local distributions of droplet radii PDFs are shown for $M = 64$, at time $t = \tau_L$: they are broad and therefore droplets with different sizes cohabit within small volumes. In fig. 5 the mean distributions are shown for $M = 1, 16, 128$. Again we observe broad distributions also for the smallest boxes we consider which is about three times the viscous scale η of our velocity field. The result shows that the broadening of the spectra is non trivial for the smallest scale we can consider.

Since the mean supersaturation is taken to be zero, a rough mean-field-type argument would yield no mean growth of droplet sizes (see eq. (3)). This prediction coincides with the classical one, which does not take into account the vapour field fluctuations. It turns out that the mean droplet size grows although the mean supersaturation value is set to zero (see fig. 6). Fluctuations thus play a crucial role for the growth of droplet radius.

To evaluate the role of inertia and sedimentation in this problem we compared the above simulations with analogous simulations where droplets are treated as fluid particles. Along Lagrangian trajectories we should observe the maximum correlation between droplets and vapour because here the supersaturation value is conserved. We would expect that inertia effects work against correlations, as they tend to deviate droplets from Lagrangian trajectories. Such effect is very weak, as we do not detect any differences between the two evolutions of the mean radius for the case with and without inertia effects (see fig. 6).

We observed no influence of inertia effects also for the segregation effect and the spreading of the size distribution. The only difference between the two simulations is visible from the evolution of mean-Lagrangian supersaturation, shown in fig. 7. From this figure we learn that in the early stage of their growth ($t/\tau_L < 0.4$) droplets are so small that inertia effects are completely negligible. They become visible (even if very weak) only at the end of the condensation stage. In view of these comparisons we can conclude that inertia and sedimentation do not change the qualitative picture of condensation we have drawn in the absence of inertia.

From the above results it turns out that turbulent fluctuations of the supersaturation field play a crucial role for droplets evolution. They allow droplets to behave in different ways

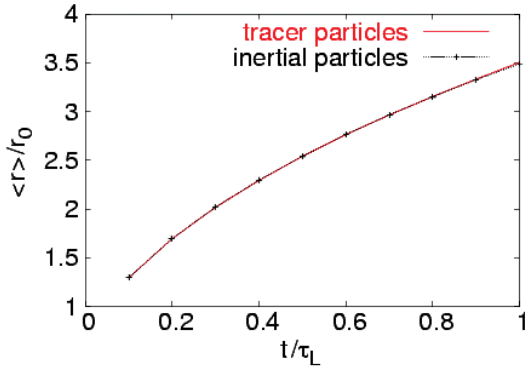


Fig. 6

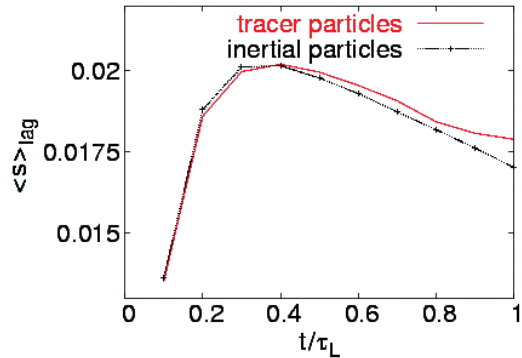


Fig. 7

Fig. 6 – Temporal evolution of $\langle r \rangle$, with $\bar{s} = 0$. The turbulent model allows the mean droplet size to grow by condensation although the Eulerian supersaturation average is set to zero. Notice that in these conditions classical models provide a constant mean droplet radius.

Fig. 7 – Mean-Lagrangian supersaturation for the model with (black curve) and without (gray, red on-line, curve) inertia effects.

depending on the particular fluctuation they experience, and lead to the segregation effect and the broadening of size spectrum.

As mentioned in the introduction, classical models of condensation in clouds focus on a single fluid parcel and do not reproduce the observed broadening of size spectra. We can now understand the reason for this shortcoming: droplets initially belonging to the same fluid parcel separate explosively and reach separations comparable with the cloud size in a time comparable with the condensation growth timescale: $t \simeq (L^2/\epsilon)^{1/3} \simeq 10^3$ s for $L = 10^3$ m and $\epsilon \sim 10^{-3} \text{ m}^2 \text{ s}^{-3}$. This makes questionable the very concept of fluid parcel. Therefore, to obtain the above results for a cloud, one should adopt a complementary point of view that consists in the simulation of the whole cloud volume. Such an approach must take into account that the spatial scales involved in atmospheric turbulence range from ≈ 1 km to ≈ 1 mm. Accordingly, the degrees of freedom in a three-dimensional turbulent flow are approximately $Re^{9/4} \approx 10^{18}$ for typical cloud conditions. It is clearly impossible to simulate a system with such a huge amount of degrees of freedom. A possible way to overcome the problem is to examine a 2D turbulent flow. Moreover from the above results one expects that the most important scales in the problem are the largest ones⁽⁴⁾. One should indeed resolve the largest scales avoiding the detailed description of small scales.

Such approach does not describe timescales small enough to be comparable with the Stokes timescale for droplets. Hence the inertia effects cannot be taken into account. Even though droplet density, ρ_d , is much larger than air density, ρ_f , that approximation is reasonable for small droplets. Indeed the Stokes number for such droplets in a turbulent flow is $St = \tau_d/\tau_f \sim (2\rho_d\epsilon^{1/2}r^2)/(9\rho_f\nu^{3/2}) \approx 0.005\text{--}0.08$ for $R \approx 5\text{--}20 \mu\text{m}$, where τ_d and τ_f are timescales associated to the droplet and to turbulent fluctuations, respectively and the numerical evaluation has been carried out for $\epsilon \sim 10^{-3} \text{ m}^2 \text{ s}^{-3}$ and $\nu \sim 10^{-5} \text{ m}^2 \text{ s}^{-1}$.

Another point that is worth emphasizing in dealing with cloud physics is that the number of droplets in a cloud reaches values of $10^{17}\text{--}10^{18}$. In the condensation stage it is not necessary to

⁽⁴⁾Furthermore, the assumption that for scales smaller than the fluid parcel scale there is no broadening and every droplet behaves in the same way seems to be reasonable according to [10].

consider this huge number of droplets because they do not interact with each other. Rather, we can follow the history of a large number of droplets which are representative of the statistical behaviour of the whole droplet population. The only drawback is that with a realistic number of droplets for a simulation the parameter τ_s is much larger than the largest timescale in the cloud. Indeed the simulated vapour field does not perceive the presence of droplets, because the sink term $-s/\tau_s$ in eq. (1) vanishes. But this is not the case of typical conditions for a developed cloud, in which the absorption time is 1–10 s (see [15]) and actually the sink term is relevant for producing vapour depletion. Therefore a way to evaluate an effective absorption timescale must be devised to reproduce the effect of droplets also on the vapour field.

* * *

This work has been supported by EU network HPRN-CT-2002-00300 and by Cofin 2003 “Sistemi Complessi e Problemi a Molti Corpi”. Numerical simulations have been performed at CINECA (INFM parallel computing initiative).

REFERENCES

- [1] MARTONEN T. B. (Editor), *Medical Applications of Computer Modeling* (WIT Press, UK) 2001.
- [2] PRUPPACHER H. R. and KLETT J. D., *Microphysics of Clouds and Precipitation* (Kluwer Academic Publishers, Boston) 1997.
- [3] ROGERS R. R. and YAU M. K., *A Short Course in Cloud Physics* (Pergamon Press, Oxford) 1989.
- [4] MALINOWSKI S. P., ZAWADZKI I. and BANAT P., *J. Atmos. Ocean. Technol.*, **15** (1998) 1060.
- [5] WARNER J., *J. Atmos. Sci.*, **26** (1969) 1049.
- [6] BRENGUIER J. L. and CHAUMAT L., *J. Atmos. Sci.*, **58** (2001) 628.
- [7] BARTLETT J. T. and JONAS P. R., *Q. J. R. Meteorol. Soc.*, **98** (1972) 150.
- [8] SHAW R. A., *Annu. Rev. Fluid Mech.*, **35** (2003) 183.
- [9] VAILLANCOURT P. A., YAU M. K. and GRABOWSKI W. W., *J. Atmos. Sci.*, **58** (2001) 1945.
- [10] VAILLANCOURT P. A., YAU M. K., BARTELLO P. and GRABOWSKI W. W., *J. Atmos. Sci.*, **59** (2002) 3421.
- [11] KOROLEV A., *J. Atmos. Sci.*, **52** (1995) 3620.
- [12] TURITSYN K., *Phys. Rev. E*, **67** (2003) 062102.
- [13] TWOMEY S., *Geofis. Pura Appl.*, **43** (1959) 243.
- [14] VAILLANCOURT P. A. and YAU M. K., *Bull. Am. Meteorol. Soc.*, **81** (2000) 285.
- [15] KHVOROSTYANOV V. I. and CURRY J. A., *J. Atmos. Sci.*, **56** (1999) 3985.